NATIONAL AERONAUTICS AND SPACE ADMINISTRATION

Technical Report 32-1283

The Influence of Several Near-Wall Injection Conditions on the Combustion Performance of a Liquid Rocket Engine

Richard M. Clayton

JET PROPULSION LABORATORY
CALIFORNIA INSTITUTE OF TECHNOLOGY
PASADENA, CALIFORNIA

September 15, 1968

NATIONAL AERONAUTICS AND SPACE ADMINISTRATION

Technical Report 32-1283

The Influence of Several Near-Wall Injection Conditions on the Combustion Performance of a Liquid Rocket Engine

Richard M. Clayton

Approved by:

D. F. Dipprey, Manager
Liquid Propulsion Section

JET PROPULSION LABORATORY
CALIFORNIA INSTITUTE OF TECHNOLOGY
PASADENA, CALIFORNIA

September 15, 1968

TECHNICAL REPORT 32-1283

Prepared Under Contract No. NAS 7-100
National Aeronautics & Space Administration

Acknowledgment

The conscientious efforts of Messrs. Jason L. Gee, Robert J. McKeon, and Thomas Egan, who acted as test conductor, test stand chief, and instrumentation technician, respectively, are gratefully appreciated. The many hours of effort by Fred G. Gerbracht on design and fabrication details is also acknowledged.

Contents

Tables

Figures

Abstract

Efforts to achieve smooth combustion and to establish steady-state behavior of a combustor under a variety of injected flow conditions have been summarized. The experimental combustion performance of an 18-in.-diam engine was found to vary under different near-wall injection conditions. Because of combustion effects, considerable spray separation is present in a main (core) flow. This separation degrades propellant mixing, especially along the outer periphery of the main flow, and produces as much as 10% performance variation, depending on the particular operating conditions of an ancillary injection scheme located near the chamber wall. A maximum performance recovery was achieved near the optimum mixture ratio for spray mixing for the boundary injector elements.

A rough combustion mode, manifested by high-amplitude disturbances of combustion pressure, was aggravated by poor stability of the streams from the boundary injection system. This condition was alleviated (but not eliminated) by modifications to the hydraulic design of the boundary system.

The Influence of Several Near-Wall Injection Conditions on the Combustion Performance of a Liquid Rocket Engine

I. Introduction

The JPL resonant combustion program has attempted to define experimentally the fully-developed wave phenomena associated with the destructive spinning mode of liquid rocket combustion instability. For the most part, previous work has dealt with 11-in.-diam engines; operating at 300-psia chamber pressure, and utilizing the Corporal,[1] the $N_2O_4 + N_2H_4$, and the $N_2O_4 +$ 50/50 ($UDMH/N_2H_4$) propellant combinations. It has been found (Refs. 1–6) that a high-amplitude, steep-fronted pressure disturbance, having many of the characteristics of a combustion-driven shock wave (i.e., detonation-like), exhibits the following features:

(1) The wave sweeps supersonically about the chamber circumference.

(2) The wave shape, velocity, and amplitude, though relatively unaffected by chamber-length changes, is affected by variations in the propellant mass flux distribution in the chamber cross section, particularly near the chamber wall.

(3) The direction of rotative travel appears to be related to the orientation of the resonance-initiating disturbance with respect to near-wall nonuniformities in the injected propellant distribution.

Based on this experimental evidence, the near-wall combustion environment appears to play a major role in the formation and sustenance of the detonation-like wave structure.

While the importance of the uniformity of propellant distribution to high thermochemical steady-state performance is recognized, and has been discussed by a number of authors, (for example, see Refs. 7–10) the effect of nonuniform conditions on nonsteady liquid rocket combustion has also been examined. This is discussed (Ref. 11) by Reardon et al. who have shown that decreasing the propellant mass flux near the outer radius of the chamber

[1]Oxidizer consists of a mixture of the following compounds with percentage by weight as noted: 81.3–84.5% HNO_3; 14.0±1.0% NO_2; 2.5±0.5% H_2O; 0.6±0.1% HF. Fuel consists of a mixture of the following compounds with percentage by weight as noted: 46.5±0.2% furfuryl alcohol ($C_4H_3OCH_2OH$); 7.0±0.2% N_2H_4; 1.5% max H_2O; 0.7% max impurities; remainder, aniline ($C_6H_5NH_2$).

cross section decreases the tendency for the development of incipient linear tangential modes of oscillations.

Of additional and perhaps greater interest to the present program is the recent work on two-phase detonations by Dabora et al. (Ref. 12). Here it was demonstrated that detonation waves are easily supported, either by fuel drops dispersed in gaseous oxidizer, or by a thin film of fuel on the wall of a detonation tube. In view of the nonlinear nature of the tangentially traveling waves known to exist in the spinning combustion mode, increased understanding of droplet/film-supported detonative processes and the role of the wall itself seems apropos.

For the JPL resonant combustion program, it was desired to extend the definition of the spinning mode to an additional combustor, which had design parameters different from those mentioned earlier. Accordingly, an injector was fabricated for an 18-in.-diam chamber to form an engine that had nominally ⅓ the propellant mass flux previously used and operated at 100 psia chamber pressure. The N_2O_4 + 50/50 propellant combination was utilized and the total flowrate to the engine was divided into two separately-manifolded and individually-controlled flows that fed main and boundary injection systems. The boundary or "barrier" injection scheme is typical of current practice in engine design. The scheme utilized for the present program provided the capability of operating over a range of near-wall conditions so that the influence of these variations on the combustion behavior of the engine could be evaluated.

Table 1. Design conditions for the 18-in.-diam engine, RC injector 1

Parameter	Main		Boundary		Overall	
	Fuel	Oxidizer	Fuel	Oxidizer	Fuel	Oxidizer
Flowrate, lbm/s	22.98	48.48	3.48	4.44	26.46	52.92
Injector Δp, psi (manifold to chamber)	129	120	108	96	—	—
Injection velocity, ft/s	86	58	92	68	—	—
Mixture ratio, $\dot{m}_o/\dot{m}_f$	2.11		1.27		2.00	
Fraction of total flow	0.90		0.10[a]		1.00	
Number of injector elements	84		24		108	

Conditions: $L^* = 41.3$ in. $\quad P_c = 100$ psia
$A_t = 127.7$ in.^{2} $\quad F_{exp} = 14{,}700$ lbf
$\epsilon_e = 2.95$ $\quad \mathcal{G} = 0.31$ lbm/s-in.^{2} $(\dot{m}_t/A_c)$
$\epsilon_c = 2.00$

[a]Defined as Z.

However, before initiating the resonant combustion experiments with this engine, it was desired to parametrically characterize its steady-state performance over a range of propellant flow conditions. Early attempts at this characterization demonstrated that the injector (designated RC injector 1) produced a relatively high performance, but the combustion experienced random roughness under certain operating conditions. The addition of face baffles prevented transitions to sustained resonance, but they had no measurable influence on the roughness, or "popping," as it has come to be known. Since smooth combustion was attainable only for limited operating conditions, and the baffles were not desired for the future resonance studies in any case, an effort to correct roughness was carried out so that future studies could utilize the experimental technique of scheduled bomb-induced resonance (Ref. 1) without the interference of spontaneous transitions.

II. Combustion Behavior of the Original Configuration

The total flowrate for RC injector 1 comprises a main (or core) flow and a boundary flow. Injector design conditions are listed in Table 1. Figure 1 illustrates its basic design and includes the composite arrangement of injector elements in the face.

The design of both elements (Fig. 1) optimizes mixing uniformity (Ref. 10) for the flow conditions listed in Table 1. The arrangement of elements in the face optimizes the nominal uniformity of axial mass flux. The lower mixture ratio of boundary flow is intended to provide relatively low-temperature reaction products adjacent to the chamber wall. This is common practice for the reduction of heat transfer in many of today's operational engines. Separate manifolds feed the propellants to the main and boundary orifices, permitting individual control over the flow conditions for either portion of the injector.

In the initial series of firings to determine combustion performance, it was discovered that the engine exhibited the popping phenomenon over a relatively wide range of boundary flow conditions, however, the actual range also depended somewhat on the main flow conditions. Eventually, a correlation of the occurrence of this rough combustion mode with the concentration of oxidizer near the chamber wall was obtained, and is summarized in Fig. 2. In these experiments, the injector incorporated face baffles that prevented sustained resonant combustion. Data points representing separate firings are plotted as main oxidizer-to-fuel ratio (r_m) vs the ratio of boundary oxidizer mass flowrate to total oxidizer mass flowrate ($\dot{m}_{bo}/\dot{m}_o$).

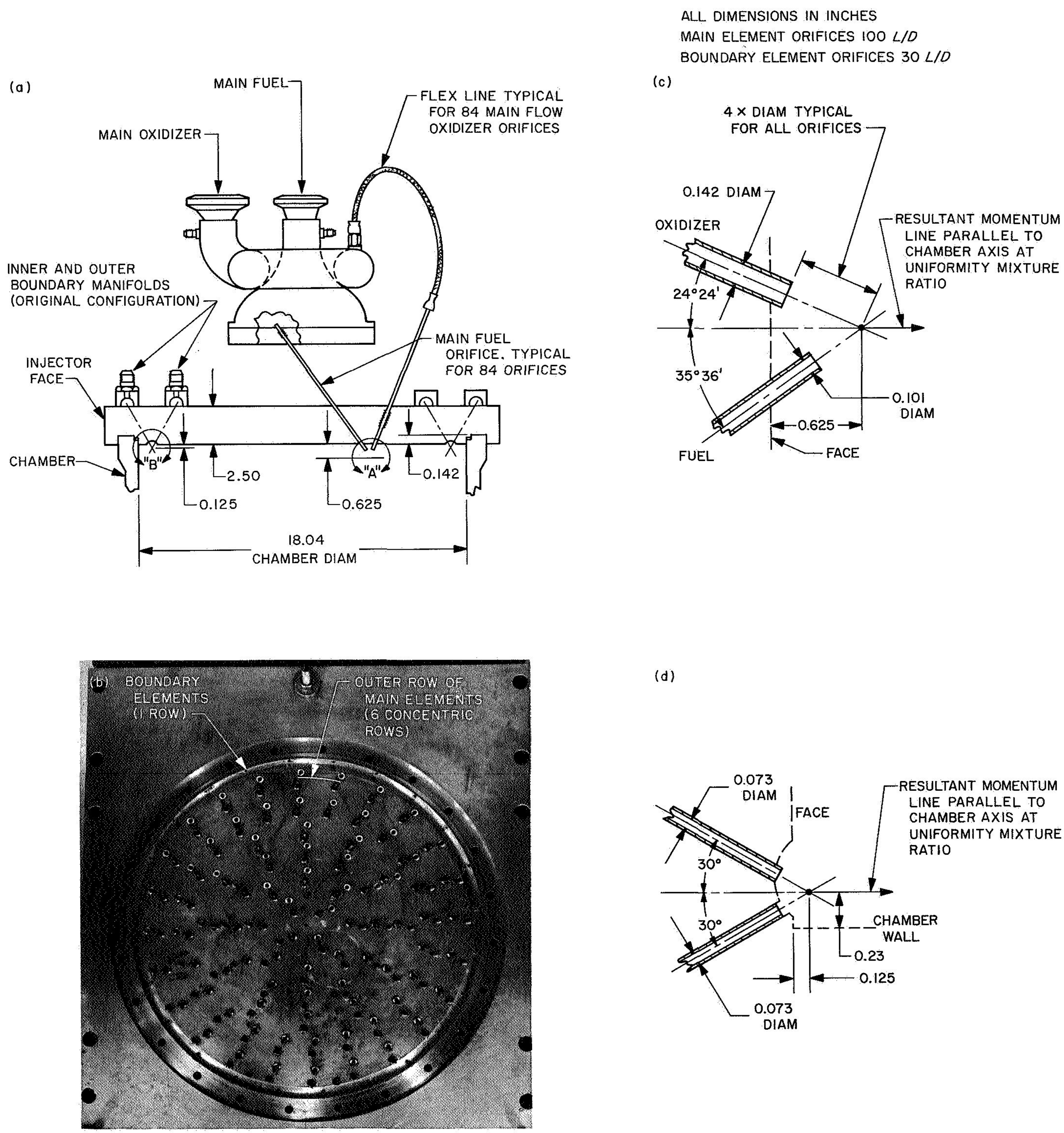

Fig. 1. RC injector 1 basic design: (a) outline drawing of engine, (b) face view of assembled injector, (c) detail of main elements (view "A"), (d) detail of boundary elements (view "B")

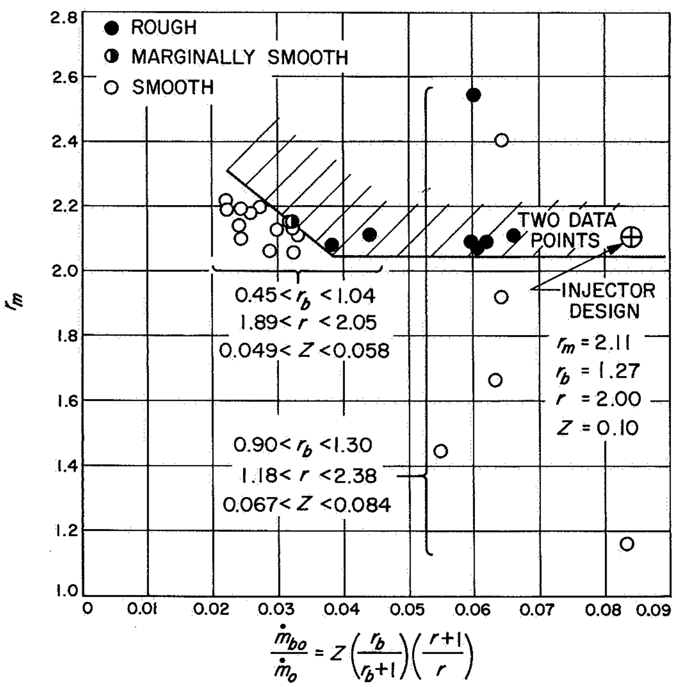

Fig. 2. Correlation of rough mode with concentration of oxidizer near the chamber wall; RC injector 1 with original boundary system

Smooth firings are shown as open circles and rough firings as solid circles. A somewhat arbitrarily positioned line separating these modes of operation is also shown. From the results, it is evident that smooth combustion was not possible at the injector design point, even though a deficiency in the test stand feed system precluded operation at precisely that point.

As a result of this behavior, it was concluded that the source of the roughness originated in the region of the chamber boundary and that it was most likely related to processes controllable by the boundary flow injection scheme. However, before attempting to correct the problem through actual injector modifications, it was decided to establish the steady-state performance of the engine in its original configuration by operating under the constraints for smooth combustion, as indicated in Fig. 2. These results are presented (Fig. 3) in terms of relative performance (uncorrected for any losses) vs overall mixture ratio. The relative performance parameters are defined as

$$\left.\begin{aligned}\eta_c &= \frac{c^*}{c^*_{th}} \times 100 \\ \eta_n &= (C_F/C_{F_{th}})_{vac} \times 100 \\ \eta &= (I_s/I_{s_{th}})_{vac} \times 100\end{aligned}\right\} \qquad (1)$$

where

η_c = relative combustion performance

η_n = relative nozzle performance

η = overall relative performance

c^* = characteristic velocity (computed from the measured flowrates and chamber pressure; nozzle entrance static pressure converted to throat stagnation conditions)

c^*_{th} = theoretical equilibrium characteristic velocity based on overall mixture ratio

C_F = thrust coefficient (computed from the measured flowrates and chamber pressure; extrapolated to vacuum conditions)

$C_{F_{th}}$ = theoretical thrust coefficient

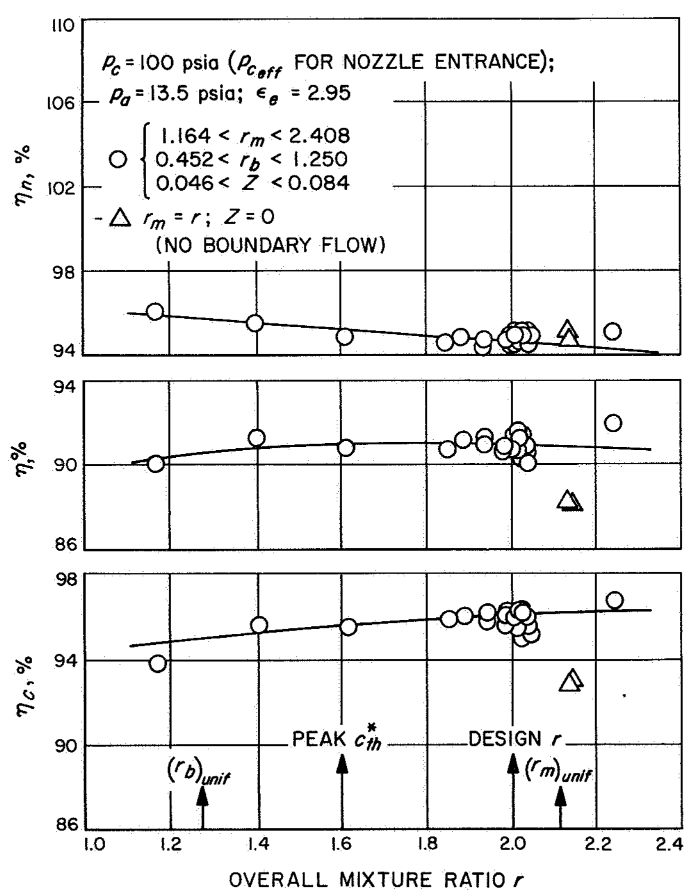

Fig. 3. Experimental relative performance of RC injector 1 with original boundary system; oxidizer near wall (runs B-914–17, -919, -926, -939, -941–944)

I_s = specific impulse (computed from measured thrust and flowrates; extrapolated to vacuum conditions)

$I_{s_{th}}$ = theoretical specific impulse

For details of typical experimental and computational methods, see Ref. 13.

The theoretical reference in each case was based on equilibrium flow at the overall mixture ratio for 100 psia chamber pressure, expanding to a vacuum through an expansion area ratio of 2.95. Computations were made with the NASA-Lewis performance program (Ref. 14) using the following heats of formation (in K cal/mole):

N_2O_4 (−4.676), N_2H_4 (12.050), UDMH (12.724)

Note in Fig. 3 that 96% of relative combustion performance (η_c) was produced by the engine near the design r value, even though the optimum boundary injection conditions could not be used. However, a substantial reduction in performance (3%) occurred when boundary flow was not used. This result was attributed to separation effects in the main sprays.

The separation phenomena was first observed at the Jet Propulsion Laboratory by Elverum and Staudhammer (Ref. 15). The very rapid reaction of N_2O_4 with N_2H_4 appeared to produce a sufficiently high rate of gas evolution that separated impinging streams of these reactants near their impingement point and prevented effective liquid-phase mixing. Later, the effect was verified quantitatively (Ref. 16) by Johnson, who measured the degradation in combustion performance of a specially designed 2000-lbf rocket combustor utilizing a single doublet-element with these same propellants. Johnson's work was extended (Ref. 17) by Evans et al., who found that the phenomena could be partly correlated with certain characteristic stream dimensions using jet or sheet types of injection elements. Finally, Kushida and Houseman (Ref. 18) attacked the problem analytically and proposed theoretical models of the separation effects.

Although the analyses of separation effects have yet to be thoroughly evaluated experimentally, existing data from the separation experiments (Refs. 15–17) offer encouraging agreement with predicted trends. In Fig. 4 results of these experiments are compared with theoretical separation criteria for the $N_2O_4 + N_2H_4$ system. Figure 4 (adapted from Ref. 18) is included here to show where the operating point of the present injector falls with respect to the theory, as well as to the previous experiments, where the separation phenomena is known to have existed.

The analysis results in two complementary criteria: one for low combustion pressure and the other for higher pressures. These are distinguished in Fig. 4 by curves labeled, respectively, liquid and gas phase reaction control. In the first case, bubbles of gas are formed as the liquid phase reactions heat the stagnated liquid interface to the boiling point, whereas in the second case, a continuous gas film is formed between the impinging liquids because of rapid gas phase reactions. In either case, the correlating parameter is termed contact time, which is defined as the ratio of stream diameter (D_j) to stream velocity (V_j) for jets; and for sheets, the ratio of sheet thickness (T_s) to sheet velocity (V_s).

If it is assumed that the separation phenomena for the N_2O_4 + 50/50 propellants are similar to those for $N_2O_4 + N_2H_4$, then both the main and the boundary elements for RC injector 1 should fall in the separation regime (Fig. 4), although a somewhat more pronounced effect should be present for the main elements. Considering the main flow injection scheme only, it is evident that the primary mixing processes for the individual elements (i.e., those processes associated with the direct impingement of the unlike streams) must suffer degradation.

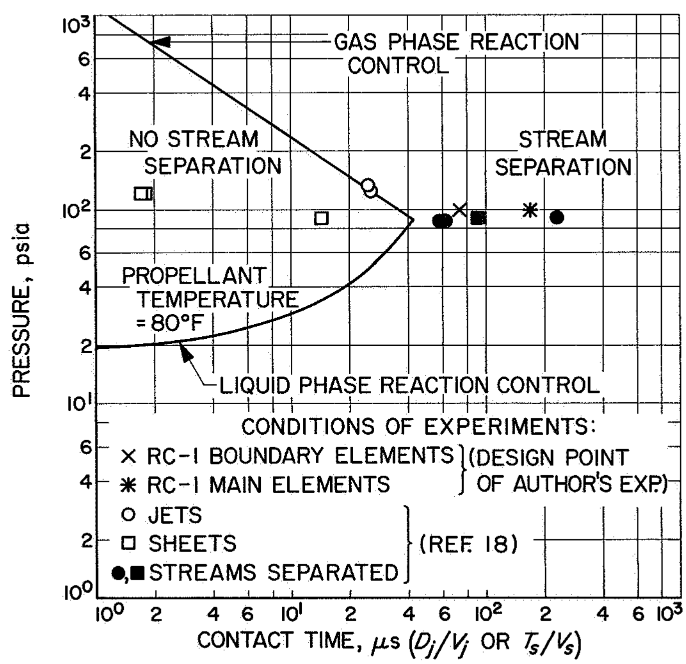

Fig. 4. Conditions of experiments plotted over theoretical separation criteria (from Ref. 18)

For the inner rows of main elements, these effects are largely counteracted by secondary mixing because of the element arrangement from row-to-row, where the oxidizer and fuel orifices for the elements are nearly adjacent in their respective rows (Fig. 1). However, for the outermost main row, separation results in an oxidizer-rich region surrounding the core reactants, since the oxidizer orifices are nearest to the chamber wall. The result is a reduction in combustion efficiency because of increased nonuniformity of overall oxidizer-to-fuel ratio, when no fuel is available to counteract the excess oxidizer in the absence of the boundary flow injection. It is further noted that the flow from the outer row of main elements constitutes over 28% of the total main flow; hence, even a small degradation of mixing in this region has a relatively large effect on the overall performance of the engine.

III. Combustion Behavior of the Revised Configuration

In view of the pronounced influence of the near-wall flow conditions on the roughness behavior of the engine, an assessment of the boundary flow injection system was undertaken. It was determined that modifications to the manifolds and orifice entries were needed to assure hydraulically stable flow conditions at the orifice exits. These modifications might curtail the rough combustion mode, lessen the constraints on operating conditions, and

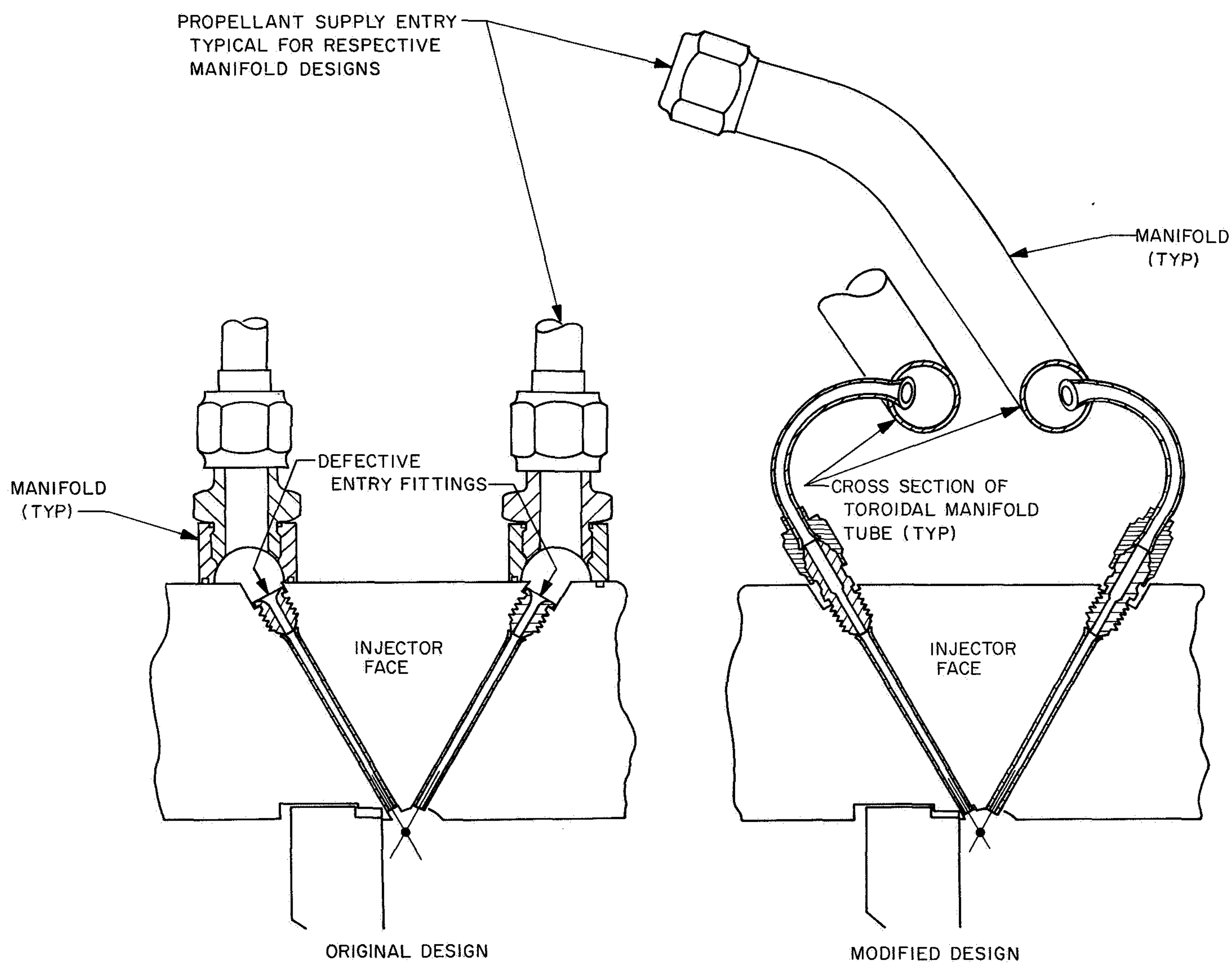

Fig. 5. Comparison of original and modified boundary inlet conditions

enable the engine to be operated at its design point without employing face baffles. Valentine et al. (Ref. 19) also attribute certain popping problems to hydraulically unstable injection schemes.

Thus, if the roughness were eliminated, it was presumed that spontaneous transitions to the resonant mode would be eliminated, but not the artificially induced (bomb) transitions. Success in eliminating roughness would then enhance the control of experimental conditions under which subsequent resonance studies could be performed. Additionally, it was felt that operation at the complete design mixture ratio would produce an increase in performance beyond the 96%, which had already been achieved. To correct the previously mentioned feed system deficiencies, test stand modifications were also incorporated. However, they affected only the capability of providing the required flow rates to the boundary manifold inlets. Changes to the manifolds and orifice entries are shown schematically in Fig. 5. Note that no changes were made to the original element geometry or to the composite arrangement of the elements in the injector face. The original three-entry-port semitoroidal manifolds were replaced by the single-port toroidal designs, as shown. The new design decreased the effective manifold volume (total volume between propellant valves and orifices) by a factor of two that, in itself, improved the starting transient flow control. However, the manifold's chief attribute was improved propellant distribution and orifice entry configuration. Photographs of the original and revised injector assemblies are shown in Fig. 6a and b, respectively. Additional details of the revised manifold are illustrated in Fig. 7, which shows one of the stepped-diameter toroidal manifolds with its feed tubes supplying the individual orifices.

When the original injector was disassembled for incorporation of the new boundary manifolds, a discrepancy in the orifice inlet fittings (Fig. 5) was also discovered. The standard AN tube fittings had been reworked to provide a contoured entry, as well as a bore to match the orifice ID (oversize in relationship to AN specifications). Unfortunately, the increased bore thinned the chamfered end of the fitting that had been inadvertently deformed during subsequent injector assembly. The entire group of early experimental firings had been made with these defective entry fittings.

This fitting problem was rectified for the revised manifold installation; however, the long entry formed by the modified feed tube arrangement apparently stabilized the injected streams even when defective orifice entry fittings

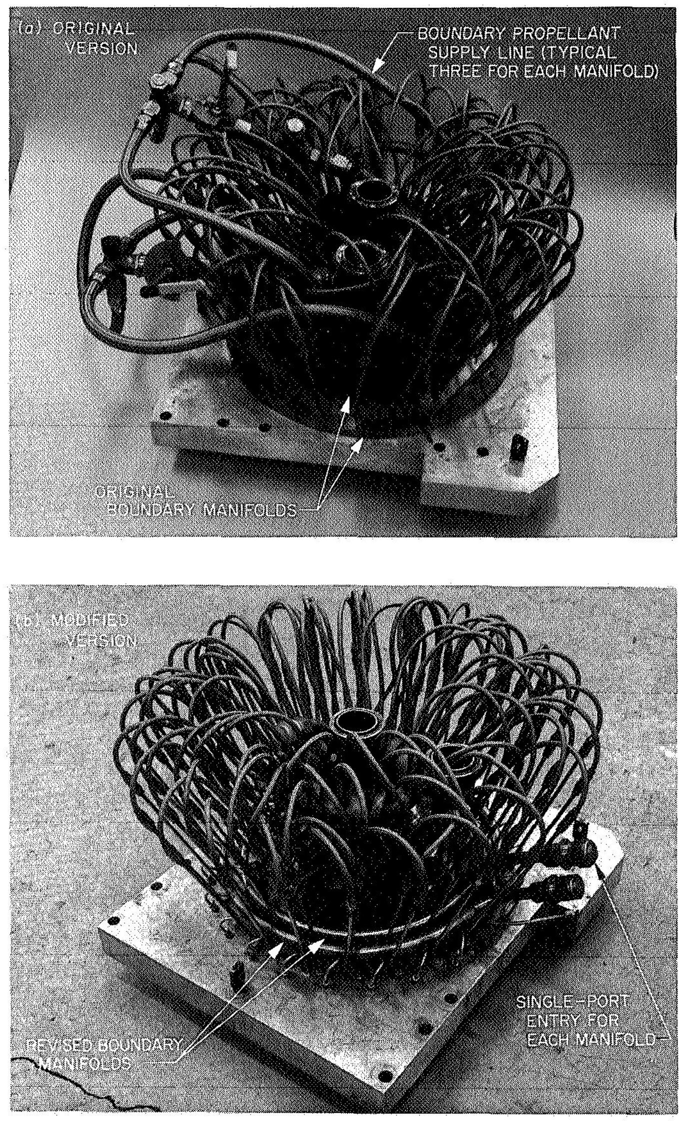

Fig. 6. RC injector 1 assembly

were retained. No disruption of a representative stream was visible when a poor fitting was used with the long-entry configuration. However, stream disruption in the form of increased spreading and directional instability was detected when the long tube entry was not employed. An orifice tube with an L/D of 30 was used in each case.

With the boundary injection system modified, as described above, and the face baffles removed, evaluation of the combustion characteristics of the engine was extended to cover the range of nominal operating conditions listed in Table 2. Figures 8 and 9 summarize the results for the boundary bipropellant orientations of oxidizer-near-wall and fuel-near-wall, respectively, where relative performance is plotted vs boundary oxidizer-to-fuel ratio,

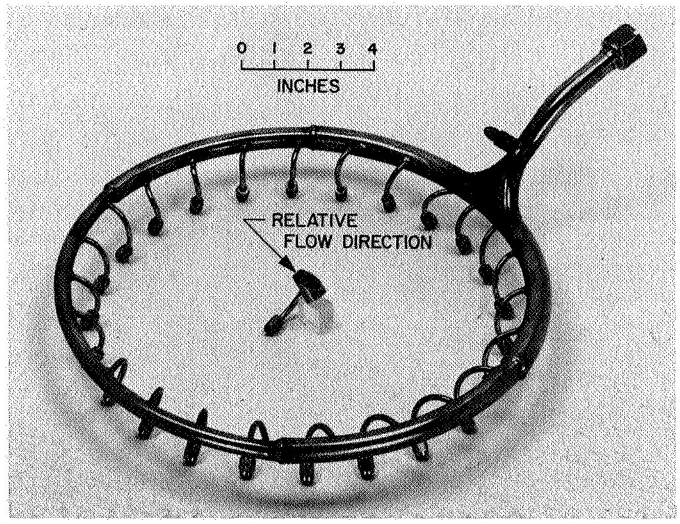

Fig. 7. Toroidal boundary manifold

with the main oxidizer-to-fuel ratio held nominally constant at its design value.

Except for the lowest value of ratio of boundary to total propellant mass flowrate (Z = 0.05), maximum relative performance was obtained near the design boundary oxidizer-to-fuel ratio for both propellant orientations. However, the oxidizer-near-wall condition yielded ~1% better performance for all conditions.

Table 2. Range of nominal operating conditions used to evaluate the combustion characteristics of the modified RC injector 1

Operating condition	Range
Main oxidizer-to-fuel ratio	Constant at design value of 2.11
Bipropellant boundary oxidizer-to-fuel ratio	0.5–2.11
Ratio of boundary to total propellant mass flowrate (Z)	0–0.15
Bipropellant boundary stream orientation (unlike impinging)	(1) Inner fuel; outer oxidizer (2) Outer fuel; inner oxidizer
Single-propellant boundary flow (like-on-like impinging)	(1) Both streams fuel (2) Both streams oxidizer

Representative data for the injector with its original boundary manifold configuration are also compared in Fig. 8. For the same operating conditions (i.e., $r_b \simeq 0.6$), the modified boundary manifolding did not change the relative performance. However, the ability to operate at the design point did improve performance by at least 1.0%. A further performance increase to approximately 98% appears possible, if the ratio of boundary to total propellant flowrate is increased to 15%.

A more convenient illustration of the effects of varying the boundary flow conditions is shown in Fig. 10, where the experimental η_c curves from Figs. 8 and 9 are com-

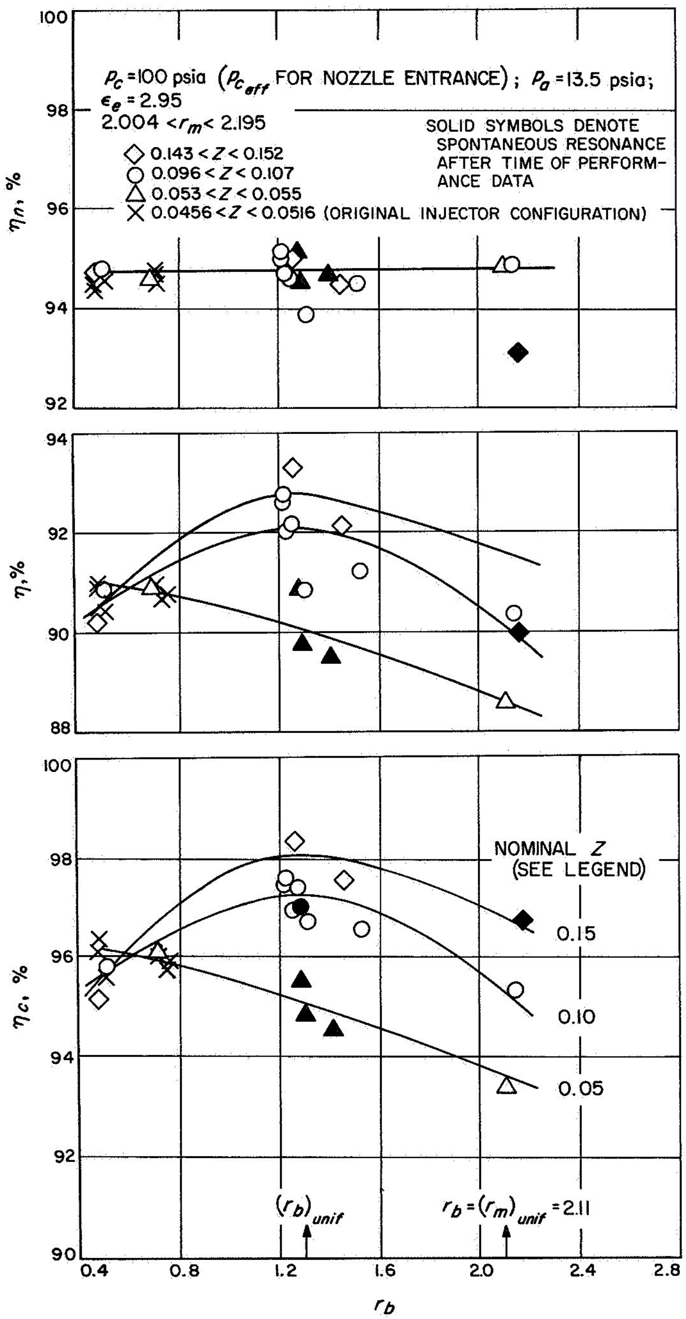

Fig. 8. Experimental relative performance of modified RC injector 1; boundary oxidizer near wall (runs B-1002, -1023, -1024, -1026–1029, -1030–1042)

pared with certain computed results and with the performance obtained for the single-propellant boundary-flow and no-boundary-flow firings. The latter condition produced the same low performance (93%) observed in the previous evaluations, whereas the oxidizer-only condition produced even lower performance. However, relative combustion performance returned to the 95–96% level, when fuel-only was injected into the boundary region.

These single-propellant results confirm the earlier conclusion that considerable degradation in mixing occurs in the periphery of the main flow through stream separation

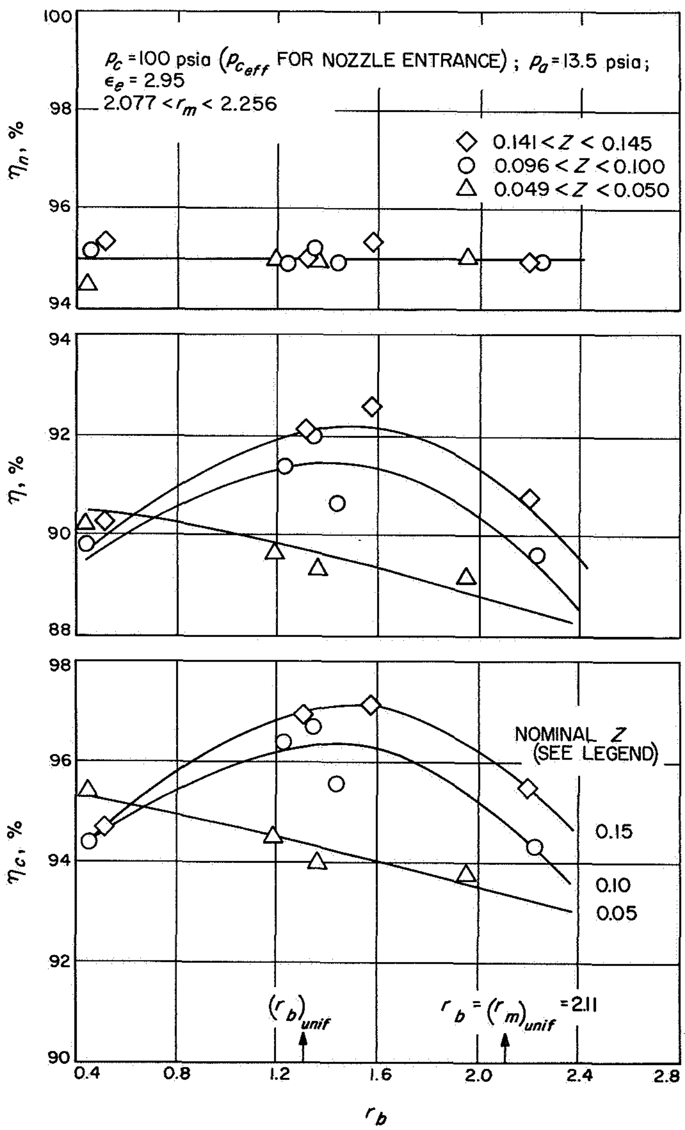

Fig. 9. Experimental relative performance of modified RC injector 1; boundary fuel near wall (runs B-1043, -1044, -1046–1049, -1060–1066)

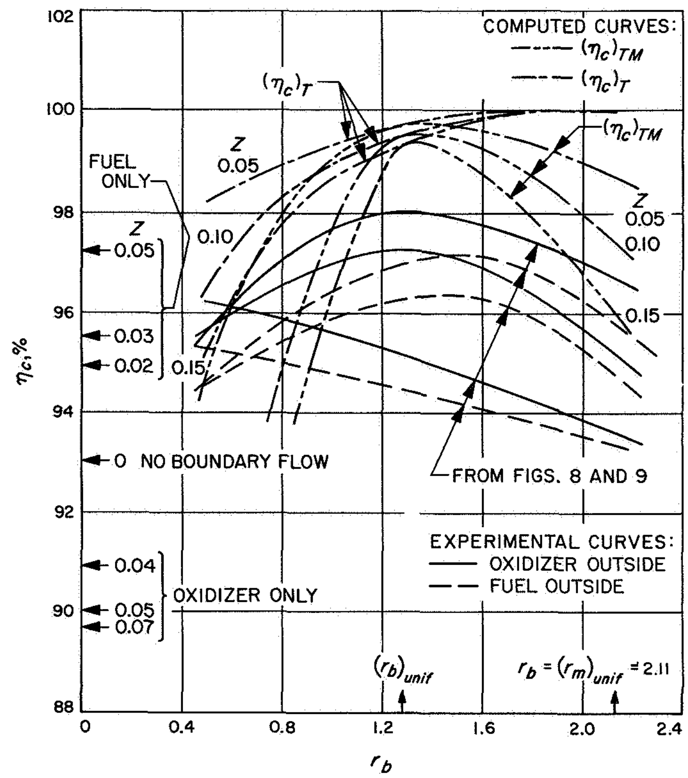

Fig. 10. Comparison of computed and experimental variation in relative combustion performance with boundary flow variation; modified RC injector 1

effects. The introduction of fuel-only into the boundary region complements the oxidizer-rich zone and enhances the relative combustion performance, whereas the injection of additional oxidizer reduces the performance.

On the other hand, the bipropellant boundary injection variations seem to yield an additional influence on overall relative performance, at least for the higher ratios of boundary to total propellant mass flowrate (Z = 0.10 and 0.15). In order to explain these trends, a simple computational model was assumed (outlined in Fig. 11) for the engine. In this model, the main and boundary flows supplied propellants to two separate zones of different oxidizer-to-fuel ratio and/or fraction of total mass flow. Each zone was presumed to react to complete thermal and chemical equilibrium according to its injected composition, with no interaction with each other. The expected thermochemical performance (c_T^*) was then approximated by the mass-weighted average theoretical performance of the two zones (Ref. 7). Thus, for nonuniform thermochemical effects only

$$c_T^* = Z\,(c_{th}^*)_b + (1 - Z)\,(c_{th}^*)_m \qquad (2)$$

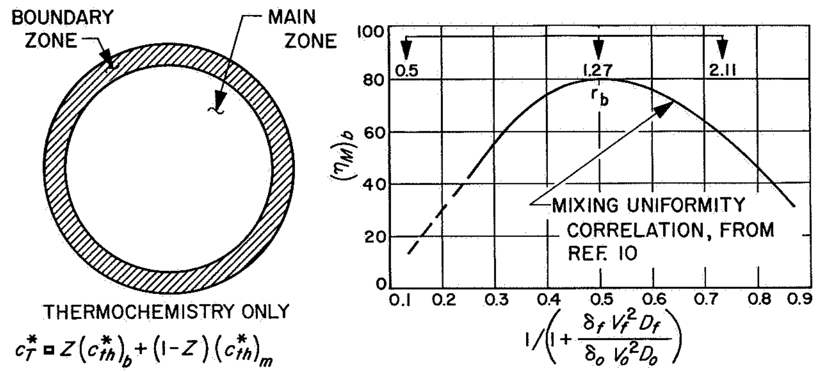

THERMOCHEMISTRY ONLY

$$c_T^* = Z(c_{th}^*)_b + (1-Z)(c_{th}^*)_m$$

FOR r_m = CONST. = 2.11

$$(c_{th}^*)_m = 5570 \text{ ft/s}$$

THUS,

$$c_T^* = Z(c_{th}^*)_b + (1-Z)(5570)$$

AND

$$(\eta_c)_T = \frac{c_T}{c_{th}^*} \times 100$$

THERMOCHEMISTRY AND VARIABLE MIXING

$$H = \frac{(\eta_M)_b}{80}$$

THUS,

$$c_{TM}^* = HZ(c_{th}^*)_b + (1-Z)(5570)$$

AND

$$(\eta_c)_{TM} = \frac{c_{TM}^*}{c_{th}^*} \times 100$$

Fig. 11. Computational model

where

c_T^* = expected characteristic velocity based on nonuniform thermochemical effects

Z = ratio of boundary to total propellant mass flowrate

c_{th}^* = theoretical equilibrium characteristic velocity based on (zone) mixture ratio

Subscripts b and m refer to boundary and main, respectively.

If it is assumed that relatively little stream separation takes place for the boundary injection elements, because of their smaller size scale (compared to the main elements), then the mixing factor, defined by Rupe (Ref. 10) and evaluated for nonreactive sprays, should apply to this reactive case. To account for degraded spray mixing due to variable boundary element mixture ratio, a normalized mixing factor is defined for the boundary elements as:

$$H = (\eta_M)_b/80 \tag{3}$$

where the mixing factor $(\eta_M)_b$ is a measure of the uniformity of mixture ratio in the resultant spray from a pair of impinging streams. Actual values for $(\eta_M)_b$ for the appropriate boundary oxidizer-to-fuel ratios are taken from the empirically derived correlation presented in Ref. 10 and plotted in Fig. 11. According to this correlation, $(\eta_M)_b$ has a maximum mean value of 80 (for the boundary element design) at the so-called uniformity mixture ratio, which occurs when the product of velocity, pressure, and diameter ratios for the doublet streams is unity.

Inserting Eq. (3) into the boundary performance term appropriately and substituting a constant value of 5570 ft/s for $(c_{th}^*)_m$ modifies Eq. (2) to include variable spray-mixing effects in the boundary flow. For these experiments, $r_m = (r_m)_{unif}$ = constant. Thus,

$$c_{TM}^* = HZ\,(c_{th}^*)_b + 5570\,(1-Z) \tag{4}$$

where

c_{TM}^* = expected characteristic velocity based on nonuniform thermochemical and degraded boundary spray mixing effects

H = normalized mixing factor

$(c_{th}^*)_b$ = theoretical equilibrium characteristic velocity based on mixture ratio for boundary flow

Computed relative combustion performance is now defined as either

$$(\eta_c)_T = \frac{c_T^*}{c_{th}^*} \times 100 \tag{5}$$

or

$$(\eta_c)_{TM} = \frac{c_{TM}^*}{c_{th}^*} \times 100 \tag{6}$$

c_{th}^* = theoretical equilibrium characteristic velocity based on overall mixture ratio

It is noted that the works of Chilenski and Lee (Ref. 19) and Sawyer (Ref. 21) show that the normally assumed chemical equilibrium compositions are not achieved with $N_2O_4 + N_2H_4$ propellants at extreme oxidizer or fuel rich mixture ratios. Therefore, caution should be used in comparing experimental data with normally computed equilibrium values when these propellants are involved. No detailed computations were made for estimating these effects for the 50/50 fuel used in the present experiments. However, considering that the range of N_2O_4/N_2H_4 ratios involved here ($1.0 < N_2O_4/N_2H_4 < 4.2$) falls generally toward the oxidizer-rich region, stated in Refs. 20 and 21, nonequilibrium effects would generally lower all values of theoretical c^*. The major influence on the present results therefore would be an upward shift of η_c values with little change to the shape (Fig. 10) of the η_c variation within the mixture ratios of interest. Thus, the use of normally computed equilibrium values to compare performance trends is assumed to be valid here.

Evaluations of Eqs. (5) and (6) over the range of conditions covered by the experiments are plotted as the uppermost (computed) sets of curves in Fig. 10. Comparison of the computed and experimental trends of performance variation with r_b indicates that inclusion of the mixing factor variation is required to predict the experimental variation and confirms that relatively little stream separation occurs with the boundary injection elements.

Evidence that some separation occurs, however, is manifested in the slightly lower performance potential of the fuel-near-wall orientation, since this orientation would direct any separated boundary oxidizer toward the already oxidizer-rich outer periphery of the main-flow reactants. Also, for variable boundary mass fraction both of the computational methods show performance trends that are opposite to the experimental trends. These facts and the singular performance curve for $Z = 0.05$ are believed to result from zone interactions, i.e., secondary mixing between the main and boundary zones that was not considered in the computations.

Because the unbaffled engine was sensitive to finite chamber pressure disturbances, spontaneous resonant combustion was encountered several times with the modified injector. The solid symbols shown in Fig. 8 indicate those firings for which transition to resonance took place after steady-state combustion had been achieved. This time of transition was a characteristic of the oxidizer-near-wall stream orientation. The triggering disturbance is presumed to have been a random "pop," since a steep-fronted high-amplitude pressure wave was generally recorded at the onset of resonance.

For the fuel-near-wall orientation, considerable difficulty was experienced in getting through the starting transient without triggering the resonant mode; however, no firing exhibited a transition once the start was successfully accomplished. For this reason, no resonant runs are plotted in Fig. 9, even though the fuel-near-wall orientation appeared to be the most unstable. Likewise, the fuel-only condition was very susceptible to transitions during start.

Definitive measurements on the fully developed resonant disturbance were not an objective of these experiments; however, sufficient high response instrumentation was used to ascertain that:

(1) The sustained resonant wave appears to be the rotating mode.

(2) No preferential rotation direction was observed.

(3) Boundary flow conditions did have a significant influence on wave amplitude, velocity, and wave form. For example, absence of boundary flow reduced the amplitude approximately 50%.

IV. Conclusions

The results of efforts to achieve smooth combustion and to establish steady-state behavior of a combustor under a variety of injected flow conditions are summarized as follows:

(1) Separation effects in reacting sprays can be a major deterrent to effective primary liquid phase mixing, but these effects can be efficiently counteracted in a multielement injection scheme by incorporating provisions for secondary mixing.

(2) Relatively large injector elements can be used, in conjunction with a limited number of smaller elements to achieve overall mixture ratio uniformity, to facilitate injector design and fabrication. This

presumes that good hydraulic design practice is exercised in the injection scheme. Regardless of combustion effects, stable and reproducible propellant stream properties are essential.

(3) In the absence of pronounced separation effects, spray mixing data for nonreactive fluids is applicable to reacting systems. With this provision, this data provides a powerful tool for injector design and for interpreting combustor behavior.

(4) One source of the popping phenomena is hydraulically unstable injection properties. Improving these properties for the near-wall injection extended the smooth-operation regime of this engine. However, a complete elimination of the popping phenomena apparently was not achieved. Although not verified here, a second source of the problem is suspected to be incipient or nonsteady stream separation which may, for instance, be a very sensitive function of propellant temperature for a given element design and propellant.

(5) The described boundary system modifications did not modify the thermochemical performance of the engine for a given off-design boundary flow condition; however, the ability to operate at the design condition did yield the improved performance expected for that operating condition.

(6) The engine is dynamically unstable without face baffles. Namely, the resonant mode is excited by nonlinear combustion pressure disturbances, but not by small fluctuations associated with combustion noise during the steady-state mode.

(7) The wave characteristics of the sustained resonant mode are significantly affected by the prevailing near-wall combustion environment—a general reduction in the severity of the wave being observed when the boundary flow is not used.

Nomenclature

A_c chamber cross sectional area

A_t nozzle throat area

c_F thrust coefficient

c^* characteristic velocity

c^*_T expected characteristic velocity based on nonuniform thermochemical effects

c^*_{TM} expected characteristic velocity based on nonuniform thermochemical and degraded boundary spray mixing effects

c^*_{th} theoretical equilibrium characteristic velocity based on overall mixture ratio

D diameter

F_{exp} experimental thrust measurement

$\mathcal{G}$ propellant mass flux

I_s specific impulse

L^* characteristic length

$\dot{m}$ mass flowrate

$\dot{m}_{bo}$ boundary oxidizer mass flowrate

$\dot{m}_f$ total fuel mass flowrate

$\dot{m}_o$ total oxidizer mass flowrate

$\dot{m}_t$ total propellant mass flowrate

p_a ambient pressure

p_c combustion pressure

r overall oxidizer-to-fuel ratio

r_b boundary oxidizer-to-fuel ratio

r_m main oxidizer-to-fuel ratio

Z ratio of boundary to total propellant mass flowrate

Δp differential pressure

ϵ_c chamber contraction area ratio

ϵ_e nozzle expansion area ratio

H normalized mixing factor

η overall relative performance

η_c relative combustion performance

Nomenclature (contd)

$(\eta_c)_T$ computed relative combustion performance based on nonuniform thermochemical effects

$(\eta_c)_{TM}$ computed relative combustion performance based on thermochemical and degraded boundary spray mixing effects

η_M mixing factor

η_n relative nozzle performance

Subscripts

b boundary

eff effective

exp experimental

f fuel

m main

o oxidizer

th theoretical

unif uniformity mixture ratio

vac vacuum

References

1. Clayton, R. M., and Rogero, R. S., *Experimental Measurements on a Rotating Detonation-Like Wave Observed During Liquid Rocket Resonant Combustion,* Technical Report 32-788, Jet Propulsion Laboratory, Pasadena, Calif., Aug. 15, 1965.
2. Clayton, R. M., and Rupe, J. H., "Resonant Combustion" in *Supporting Research and Advanced Development,* Space Programs Summary 37-30, Vol. IV, pp. 123–130, Jet Propulsion Laboratory, Pasadena, Calif., Dec. 31, 1964.
3. Clayton, R. M., and Sotter, J. G., "Resonant Combustion" in *Supporting Research and Advanced Development,* Space Programs Summary 37-36, Vol. IV, pp. 163–173, Dec. 31, 1965.
4. Clayton, R. M., et al., "Resonant Combustion" in *Supporting Research and Advanced Development,* Space Programs Summary 37-41, Vol. IV, pp. 134–151, Oct. 31, 1966.
5. Clayton, R. M., and Sotter, J. G., "Resonant Combustion" in *Supporting Research and Advanced Development,* Space Programs Summary 37-42, Vol. IV, pp. 88–103, Dec. 31, 1966.
6. Clayton, R. M., "Resonant Combustion" in *Supporting Research and Advanced Development,* Space Programs Summary 37-43, Vol. IV, pp. 224–230, Feb. 31, 1967.
7. Wrobel, J. R., "Some Effects of Gas Stratification on Choked Nozzle Flows," *J. Spacecraft and Rockets,* Vol. 2, No. 6, pp. 918–922, Dec. 1965.
8. Hersch, M., *A Mixing Model for Rocket Engine Combustion,* NASA TN D-2881. National Aeronautics and Space Administration, Lewis Research Center, Cleveland, Ohio, June 1965.
9. Pieper, J. L., Dean, L. E., and Valentine, R. S., "Effect of Mixture Ratio Distribution on Rocket I_{SP}," *J. Spacecraft and Rockets,* Vol. 4, No. 6, pp. 786–789, June 1967.

References (contd)

10. Rupe, J. H., *An Experimental Correlation of the Nonreactive Properties of Injection Schemes and Combustion Effects in a Liquid-Propellant Rocket Engine: Part I The Application of Nonreactive-Spray Properties to Rocket-Motor Injector Design.*, Technical Report 32-255, Jet Propulsion Laboratory, Pasadena, Calif., July 15, 1965.

11. Reardon, F. H., McBride, J. M., and Smith, A. J., "Effect of Injection Distribution on Combustion Stability," *J. Spacecraft and Rockets,* Vol. 4, No. 3, pp. 506–512, Mar. 1966.

12. Dabora, E. K., Raglund, K. W., and Ranger, A. A., *Two Phase Detonations and Drop Shattering Studies,* NASA CR-72225, University of Michigan, Ann Arbor, Mich., Apr. 1967.

13. Clayton, R. M., Rupe, J. H., and Gerbracht, F. G., *An Experimental Correlation of the Nonreactive Properties of Injection Schemes and Combustion Effects in a Liquid Propellant Rocket Engine. Part II: Experimental Apparatus and Techniques,* Technical Report 32-255, Jet Propulsion Laboratory, Pasadena, Calif., May 15, 1967.

14. Zeleznik, F. J., and Gordon S., *A General IBM 704 or 7090 Computer Program for Computation of Chemical Equilibrium Compositions, Rocket Performance, and Chapman-Jouguet Detonations.* NASA TN-D1454. National Aeronautics and Space Administration, Washington, 1962.

15. Elverum, G. W., Jr., and Staudhammer, P., The *Effect of Rapid Liquid-Phase Reactions on Injector Design and Combustion in Rocket Motors,* Progress Report 30-4, Jet Propulsion Laboratory, Pasadena, Calif., Aug. 25, 1959.

16. Johnson, B. H., *An Experimental Investigation of the Effects of Combustion on the Mixing of Highly Reactive Liquid Propellants,* Technical Report 32-689, Jet Propulsion Laboratory, Pasadena, Calif., July 15, 1965.

17. Evans, D. D., Stanford, H. B., and Riebling, R. W., *The Effect of Injector-Element Scale on the Mixing and Combustion of Nitrogen Tetroxide-Hydrazine Propellants,* Technical Report 32-1178, Jet Propulsion Laboratory, Pasadena, Calif., Nov. 1, 1967.

18. Kushida, R., and Houseman, J., *Criteria for Separation of Impinging Streams of Hypergolic Propellants,* Paper WSCI-67-38, presented at Fall Meeting of Western States Section/Combustion Institute, Seattle, Wash., Oct. 30–31, 1967.

19. Valentine, R. S., Rossi, F. S., and Kromrey, R. V., "Fluid Dynamic Effects on Apollo Engine Pressure Spikes," *AIAA J. Spacecraft and Rockets,* Vol. 5, No. 1, pp. 31–35, Jan. 1968.

20. Chelenski, J. J., and Lee, D. H., *An Experimental Investigation of the Performance of the Nitrogen Tetroxide-Hydrazine System in the Oxidizer-Rich and Fuel-Rich Regions,* Technical Report 32-212, Jet Propulsion Laboratory, Pasadena, Calif., Mar. 12, 1962.

21. Sawyer, R. F., "Theoretical Effect of Nonequilibrium Combustion on N_2H_4/N_2O_4 Propellant Performance," *J. Spacecraft and Rockets,* Vol. 5, No. 1, pp. 116–117, Jan. 1968.